

Nonperturbative thermodynamic extrinsic curvature of the anyon gas

Mahnaz Tavakoli Kachi ^{*}, Behrouz Mirza [†] and Fatemeh Sadat Hashemi [‡]

*Department of Physics,
Isfahan University of Technology,
Isfahan 84156-83111, Iran*

Thermodynamic extrinsic curvature is a new mathematical tool in thermodynamic geometry. By using the thermodynamic extrinsic curvature, one may obtain a more complete geometric representation of the critical phenomena and thermodynamics. We introduce nonperturbative thermodynamic extrinsic curvature of an ideal two dimensional gas of anyons. Using extrinsic curvature, we find new fixed points in nonperturbative thermodynamics of the anyon gas that particles behave as semions. Here, we investigate the critical behavior of thermodynamic extrinsic curvature of two-dimensional Kagome Ising model near the critical point $\beta_c = (k_B T_c)^{-1}$ in a constant magnetic field and show that it behaves as $|\beta - \beta_c|^\alpha$ with $\alpha = 0$, where α denotes the critical exponent of the specific heat. Then, we consider the three dimensional spherical model and show that the scaling behavior is $|\beta - \beta_c|^\alpha$, where $\alpha = -1$. Finally, using a general argument, we show that extrinsic curvature K have two different scaling behaviors for positive and negative α . For $\alpha > 0$, our results indicate that $K \sim |\beta - \beta_c|^{\frac{1}{2}(\alpha-2)}$. However, for $\alpha < 0$, we found a different scaling behavior, where $K \sim |\beta - \beta_c|^\alpha$.

Keywords: Thermodynamic extrinsic curvature; Anyon gas; Semions; Spherical Ising model.

1. Introduction

Weinhold introduced a geometrical metric based on the Hessian matrix of the internal energy [1]. However, he did not investigate the distance between the thermodynamic states. Ruppeiner introduced a metric and suggested a correspondence between the singularities that appears in thermodynamic geometry and phase transitions [2, 3]. A proof of the correspondence was proposed in [4, 5]. It was suggested by Ruppeiner that the sign of the thermodynamic scalar curvature may determine the character of the microscopic interaction, whether it is repulsive ($R < 0$) or attractive ($R > 0$). The thermodynamic scalar curvature R of the ideal gas is equal to zero ($R = 0$) [2]. The scalar curvature can be used as a new tool to measure the amount of interaction among microstates.

So far, the thermodynamic geometry of various systems has been obtained. For a review of those models, see [6]. Janyszek and Mrugala have obtained the thermodynamic scalar curvature of ideal quantum gases [7]. The results show that R

^{*}m.tavakoli1386@ph.iut.ac.ir

[†]b.mirza@iut.ac.ir

[‡]hashemifatemeh038@gmail.com

is negative for a gas of Fermions and is positive for a Bose gas. Thermodynamic geometry of an anyon gas which obeys fractional statistics has been investigated via the thermodynamic scalar curvature R and some notable aspects of anyon gas has been reported [8, 9]. The scalar curvature of anyons has both signs, whose change from positive (Bose like behavior) to negative values (Fermi like gas).

Near the critical point, both correlation length ξ and the thermodynamic curvature R diverge. It was suggested and confirmed in different studies that near the critical point the thermodynamic scalar curvature can be written as $R \sim \kappa \xi^d$, where d is dimension of the system, ξ is the correlation length and κ is a constant [2, 3, 10–14]. Considering the scaling relation $\nu d = 2 - \alpha$ where α and ν are critical exponents, the thermodynamic curvature behaves as $R \sim t^{\alpha-2}$ where t denotes the difference in the temperature from its critical value, $t = \beta - \beta_c$. Therefore, using the scaling behavior of R , the critical exponent of the thermodynamic system can be investigated, e.g. the scaling behavior of the thermodynamic scalar curvature for three dimensional Van-der Waals model and four dimensional spherical model is $R \sim t^{\alpha-2}$ ($\alpha = 0$) [15]. While the critical behavior of thermodynamic scalar curvature of two dimensional Kagome Ising model is $R \sim t^{\alpha-1}$, where $\alpha = 0$ [11]. Therefore, we expect that in some cases the scaling behavior of R depends on the dimension of thermodynamic system.

Thermodynamic geometry of black holes may give us useful information about their microstates interactions [16]. It was suggested that microstates in the Kerr-Newman black holes might behave as fermions and represent repulsive interactions [17, 18]. Also, it was found that the critical exponents of the Van der Waals fluid are the same as that of the charged AdS black holes [19–21].

Among these, an interesting subject is to investigate thermodynamic extrinsic curvature in statistical systems. The inspiration of this work is the earlier study of black holes thermodynamic geometry by using the extrinsic curvature [22]. The results indicate the correspondence between the singularities of the thermodynamic extrinsic curvature and the phase transition points that are corresponded to the heat capacity. The thermodynamic extrinsic curvature could be an important geometrical quantity in the study of critical phenomena. In this work we start to investigate the following issues. Whether the extrinsic curvature on an embedded hypersurface in the thermodynamic manifold can provide useful information about critical phenomenon. Does the scaling behavior of the thermodynamic extrinsic curvature depends on the dimension? What type of universal behaviors and information may be obtained study of the thermodynamic extrinsic curvature. To explore usefulness of thermodynamic extrinsic curvature, we study some statistical systems in the following sections. In this paper, we study the critical behavior of the gas of anyons and two critical spin systems by using thermodynamic extrinsic curvature. We derive the thermodynamic extrinsic curvature and compare its properties with the well known thermodynamic Ricci scalar.

This paper is outlined as follows. In section 2, we review some of the basic relations in the thermodynamic geometry. In section 3, we first briefly present the

thermodynamic properties of an anyon gas which obeys fractional statistics and obtain its thermodynamic extrinsic curvature. In section 4, we consider thermodynamic geometry of two dimensional Kagome Ising model and find the critical exponent using the extrinsic curvature. We also explore thermodynamic geometry of three dimensional spherical model. The standard scaling behavior of the extrinsic curvature is given in 5. A summary of the results can be found in section 6. Details on relations of the Kagome Ising model can be reached in Appendix.

2. Thermodynamic geometry

Weinhold and Ruppeiner introduced a geometrical formulation of thermodynamic [1, 2]. Weinhold suggested the energy representation by using the internal energy and its second derivative. Ruppeiner introduced the metric by the second derivative of entropy. It was suggested that both formulations are equivalent and the metrics are related by a conformal transformation [23]. Using Legendre transformations one may generate other forms of thermodynamic metrics. A new form of thermodynamic metric was recently proposed in [4]. In 1990, Janyszek and Mrugala used logarithm of the partition function and its second derivative to generate a metric for geometric formulation of thermodynamic as follows [7]

$$g_{ij} = \frac{\partial^2 \ln Z}{\partial \beta_i \partial \beta_j}, \quad (1)$$

where $\beta_i = \frac{1}{k_B} \frac{\partial S}{\partial X_i}$, S is the entropy and X_i denote the extensive parameters of the thermodynamic systems (in the following sections we use both Latin and Greek indices for the metric components). Then, one may calculate other geometrical quantities such as the scalar and the extrinsic curvatures. The thermodynamic scalar curvature in a two dimensional space is determined as follows

$$R = \frac{\begin{vmatrix} g_{11} & g_{22} & g_{12} \\ g_{11,1} & g_{22,1} & g_{12,1} \\ g_{11,2} & g_{22,2} & g_{12,2} \end{vmatrix}}{2 \begin{vmatrix} g_{11} & g_{12} \\ g_{21} & g_{22} \end{vmatrix}^2}, \quad (2)$$

where the parameters of the thermodynamic space are (β_1, β_2) and $g_{ij,k} = \frac{\partial g_{ij}}{\partial X_k}$. It was argued that curvature singularities which are roots of the denominator of R are corresponded to the second order phase transitions [4, 5]. So far, most of attempts in thermodynamic geometry of statistical systems were in the context of scalar curvature. However, recently the extrinsic curvature was introduced as a new tool in thermodynamic geometry [22]. It was shown that the extrinsic curvature plays a key role in determining the stability of the thermodynamic system. Here, we are going to use extrinsic curvature to study the critical behaviour of some statistical systems.

In the following lines, we review definition of extrinsic curvature in differential geometry. A hypersurface Σ can be defined by a restriction on coordinates $\mathcal{H}(X^a) = 0$, where X^a are coordinates. The extrinsic curvature is expressed as

$$K = \nabla_\mu \tilde{n}^\mu = \frac{1}{\sqrt{g}} \partial_\mu (\sqrt{g} \tilde{n}^\mu), \quad (3)$$

where g denotes the determinant of the metric and \tilde{n}_μ is a normal vector to hypersurface Σ . The normalized vector \tilde{n}_μ is given by

$$\tilde{n}_\mu = \frac{\partial_\mu \mathcal{H}}{\sqrt{g^{\mu\nu} \partial_\mu \mathcal{H} \partial_\nu \mathcal{H}}}. \quad (4)$$

In this paper, we deal with two dimensional thermodynamic manifolds therefore each hypersurface refers to a one-dimensional curve. In the following, we investigate the extrinsic curvature of anyon gas, two dimensional Kagome Ising model and the spherical model. We elaborate on new aspects of using the extrinsic curvature in thermodynamic geometry.

3. Anyon gas

In this section, our main goal is to derive the nonperturbative thermodynamic extrinsic curvature of an anyon gas and compare its thermodynamic behavior with the corresponding scalar curvature obtained in [8, 9].

It is known that in $3 + 1$ dimensions states of identical bosons (fermions) are symmetric (antisymmetric) under the interchange of particles. However, the interchange of two identical particles in $2 + 1$ dimensions may produce an arbitrary phase $e^{i\pi\alpha}$. The statistical parameter α is in the range $0 \leq \alpha \leq 1$ where, $\alpha = 0, 1$ corresponds to bosons and fermions, respectively. The particles with fractional statistics ($0 < \alpha < 1$) were called anyons by Wilczek [24]. Over the years, much works have been done to investigate anyons [24–27]. Although fractional exchange statistics mostly defined in two dimensional space, it may also be appear in $d = 1$ [28, 29]. Another type of fractional statistics is fractional exclusion statistic that was introduced by Haldane [25]. Fractional exclusion statistic is based on Hilbert space and therefore can be defined for an arbitrary dimension $d \geq 2$ [30–34].

In this section, we will obtain the thermodynamic extrinsic curvature of an anyon gas obeying fractional exclusion statistics. To do this, we first briefly review the thermodynamic formulation of the anyon gas [35–37]. Wu formulated the statistical distribution of anyons by using Haldane’s fraction exclusion statistics as follows [27]

$$n_i = \frac{1}{w(\exp \left[\frac{\varepsilon_i - \mu}{k_B T} \right]) + \alpha}, \quad (5)$$

where, μ denotes the chemical potential of anyons and ε is the energy of the single particle. The function $w(\chi)$ fulfills a certain functional equation, $w(\chi)^\alpha [1 + w(\chi)^{1-\alpha}] = \chi$ where, $w(\chi) = \chi - 1$ for bosons ($\alpha = 0$) and for fermions ($\alpha = 1$),

$w(\chi) = \chi$. In the classical limit ($\exp[\frac{\varepsilon_i - \mu}{k_B T}] \gg 1$), we have $w(\chi) = \chi + \alpha - 1$ therefore the particle number and the internal energy of anyons are given by

$$\begin{aligned} N &= \sum_i n_i = \sum_i \frac{1}{\exp[\frac{\varepsilon_i - \mu}{k_B T}] + 2\alpha - 1}, \\ U &= \sum_i n_i \varepsilon_i = \sum_i \frac{\varepsilon_i}{\exp[\frac{\varepsilon_i - \mu}{k_B T}] + 2\alpha - 1}. \end{aligned} \quad (6)$$

The above particle number and internal energy reduce to boson and fermion cases by choosing $\alpha = 0$ and $\alpha = 1$, respectively. It was proposed by Huang that a system of N particles with both α fractions of fermions and $(1 - \alpha)$ fractions of bosons can establish anyon statistics [36]. Therefore, Based on the Huang's factorized method, the thermodynamic quantity $Q(\alpha)$ can be written as

$$Q_{\text{anyon}} = \alpha Q_{\text{fermion}} + (1 - \alpha) Q_{\text{boson}}. \quad (7)$$

As a consequence, the particle number and the internal energy of the anyons can be written as the combination of the particle number and the internal energy of fermions and bosons. Moreover, at finite temperatures for N particle number of anyons in the volume V with a mass m we have [27]

$$\frac{\mu_a}{k_B T} = \frac{\alpha h^2}{2\pi m k_B T} \frac{N}{V} + \ln \left(1 - \exp\left[\frac{-h^2}{2\pi m k_B T} \frac{N}{V}\right] \right). \quad (8)$$

By rewriting Eq. (8) for boson ($\alpha = 0$), fermion ($\alpha = 1$) and assuming that $N_a = N_b = N_f = N$ we arrive at

$$\mu_a = \alpha \mu_f + (1 - \alpha) \mu_b, \quad (9)$$

which is compatible with the factorized property (Eq.(7)), where a , f and b indices means anyon, fermion and boson, respectively. Therefore, the fugacity of anyons is written as $z_a = z_f^\alpha z_b^{(1-\alpha)}$ where

$$\begin{aligned} z_b &= \exp\left[\frac{\mu_b}{k_B T}\right] = (1 - \exp\left[\frac{-N_b \beta}{y}\right]), \\ z_f &= \exp\left[\frac{\mu_f}{k_B T}\right] = \exp\left[\frac{\alpha N_f \beta}{y}\right] (1 - \exp\left[\frac{-N_f \beta}{y}\right]), \\ z_a &= \exp\left[\frac{\mu_a}{k_B T}\right] = \exp\left[\frac{\alpha N_a \beta}{y}\right] (1 - \exp\left[\frac{-N_a \beta}{y}\right]), \end{aligned} \quad (10)$$

where $\beta = \frac{1}{k_B T}$ and $y = \frac{2\pi m V}{h^2}$. In the following, we consider two dimensional space. Therefore, for two dimensional momentum space we replace the summation with $\frac{2\pi m V}{h^2} \int_0^\infty d\varepsilon$ in Eq. (6). Then, the particle number and the internal energy of anyons are given by [9]

$$\begin{aligned} N_a &= y \beta^{-1} (\alpha \ln(1 + z_f) - (1 - \alpha) \ln(1 - z_b)), \\ U_a &= y \beta^{-2} (-\alpha Li_2(-z_f) + (1 - \alpha) Li_2(z_b)), \end{aligned} \quad (11)$$

where $Li_n(x)$ represents the polylogarithm function. To simplify the relations, we set $y = 1$. Considering Eq.(11) the parameter space is (β, γ_i) , where $\gamma_i = -\frac{\mu_i}{k_B T}$. The metric elements of boson gas, fermion gas and anyon gas can be obtained via Eq. (1) where $Z(\beta, \gamma_i) = Tr \exp[-\beta H - \gamma_i N]$ and $\langle H \rangle = U$. Therefore, using Eq.(11), the metric elements for the ideal boson gas ($\alpha = 0$) with the parameters of (β, γ_b) is written as

$$\begin{aligned} (g_b)_{\beta\beta} &= \frac{\partial^2 \ln(Z_b)}{\partial \beta^2} = -\left(\frac{\partial U_b}{\partial \beta}\right)_{\gamma_b} = 2\beta^{-3} Li_2(z_b), \\ (g_b)_{\beta\gamma_b} &= (g_b)_{\gamma_b\beta} = \frac{\partial^2 \ln(Z_b)}{\partial \gamma_b \partial \beta} = -\left(\frac{\partial U_b}{\partial \gamma_b}\right)_{\gamma_b} = -\beta^{-2} \ln(1 - z_b), \\ (g_b)_{\gamma_b\gamma_b} &= \frac{\partial^2 \ln(Z_b)}{\partial \gamma_b \partial \gamma_b} = -\left(\frac{\partial N_b}{\partial \gamma_b}\right)_{\beta} = \beta^{-1} \frac{z_b}{1 - z_b}, \end{aligned} \quad (12)$$

and the metric elements of the ideal fermion gas ($\alpha = 1$) with the parameters (β, γ_f) are as follows

$$\begin{aligned} (g_f)_{\beta\beta} &= \frac{\partial^2 \ln(Z_f)}{\partial \beta^2} = -\left(\frac{\partial U_f}{\partial \beta}\right)_{\gamma_f} = -2\beta^{-3} Li_2(-z_f), \\ (g_f)_{\beta\gamma_f} &= (g_f)_{\gamma_f\beta} = \frac{\partial^2 \ln(Z_f)}{\partial \gamma_f \partial \beta} = -\left(\frac{\partial U_f}{\partial \gamma_f}\right)_{\gamma_f} = \beta^{-2} \ln(1 + z_f), \\ (g_f)_{\gamma_f\gamma_f} &= \frac{\partial^2 \ln(Z_f)}{\partial \gamma_f \partial \gamma_f} = -\left(\frac{\partial N_f}{\partial \gamma_f}\right)_{\beta} = \beta^{-1} \frac{z_f}{1 + z_f}. \end{aligned} \quad (13)$$

Then, the metric elements of anyon takes the following form

$$\begin{aligned} (g_a)_{\beta\beta} &= \frac{\partial^2 \ln(Z_a)}{\partial \beta^2} = -\left(\frac{\partial U_a}{\partial \beta}\right)_{\gamma_a} = 2\beta^{-3}(-\alpha Li_2(-z_f) + (1 - \alpha) Li_2(z_b)), \\ (g_a)_{\beta\gamma_a} &= (g_a)_{\gamma_a\beta} = \frac{\partial^2 \ln(Z_a)}{\partial \gamma_a \partial \beta} = -\left(\frac{\partial N_a}{\partial \beta}\right)_{\gamma_a} = \beta^{-2}(\alpha \ln(1 + z_f) - (1 - \alpha) \ln(1 - z_b)), \\ (g_a)_{\gamma_a\gamma_a} &= \frac{\partial^2 \ln(Z_a)}{\partial \gamma_a \partial \gamma_a} = -\left(\frac{\partial N_a}{\partial \gamma_a}\right)_{\beta} = \frac{-1}{\left(\frac{\partial N_a}{\partial \gamma_a}\right)_{\beta}} \\ &= \beta^{-1} \frac{z_f z_b}{2\alpha z_f z_b + \alpha z_b - \alpha z_f - z_f z_b + z_f}. \end{aligned} \quad (14)$$

Also, It is known that in the calssical limit, the equation of state takes the following form [27]

$$PV = Nk_B T \left(1 + (2\alpha - 1) \frac{N\lambda^2}{4V}\right), \quad (15)$$

where $\lambda = \frac{h}{\sqrt{2\pi m k_B T}}$. Therefore, the interaction is repulsive for $\alpha > \frac{1}{2}$ and is attractive for $\alpha < \frac{1}{2}$. For $\alpha = \frac{1}{2}$ an ideal equation of state is reached [8]. Nonperturbative

thermodynamic geometry of anyon gas was investigated in [9]. It was found that the scalar curvature has opposite signs for boson ($R > 0$) and fermion ($R < 0$) cases [7, 8]. It is known that the positive scalar curvature indicates the attractive interaction while the negative one leads to repulsive interaction [6, 8]. Moreover, at the Bose-Einstein condensation the corresponding thermodynamic scalar curvature diverges. It was shown that anyons behave as an ideal classical gas at $\alpha = \frac{1}{2}$ where $R = 0$ [8]. For a thorough discussion, the interested reader is referred to [9].

Now, we will compute the thermodynamic extrinsic curvature of bosons, fermions and anyon gas. We assume a constant hypersurface, $\beta = cte$, in order to compare the results with thermodynamic properties obtained via thermodynamic scalar curvature for an isotherm in [9]. The starting point is to compute a normal vector of the hypersurface. So, using Eq.(4) and Eq.(12) the normal vector $(\tilde{n}_b)_\beta$ for bosons is given by

$$\begin{aligned} (\tilde{n}_b)_\beta &= \frac{\partial_\beta \mathcal{H}}{\sqrt{(g_b)^{\beta\beta} \partial_\beta \mathcal{H} \partial_\beta \mathcal{H}}} \\ &= \frac{1}{\sqrt{(g_b)^{\beta\beta}}} = \left(\frac{2z_b Li_2(z_b) + (z_b - 1) \ln(1 - z_b)^2}{\beta^3 z_b} \right)^{\frac{1}{2}}, \end{aligned} \quad (16)$$

it should be noted that another component $((\tilde{n}_b)_{\gamma_b})$ is equal to zero. For fermions using the same calculations we have

$$(\tilde{n}_f)_\beta = \frac{1}{\sqrt{(g_f)^{\beta\beta}}} = \left(-\frac{2z_f Li_2(-z_f) + (z_f + 1) \ln(z_f + 1)^2}{\beta^3 z_f} \right)^{\frac{1}{2}}, \quad (17)$$

where we have used Eq.(13), and the other component $((\tilde{n}_f)_{\gamma_f})$ is equal to zero. The normal vector with upper indices has both components $((\tilde{n}_i)^\beta$ and $(\tilde{n}_i)^{\gamma_i})$ due to the off-diagonal metrics (Eqs.(12), (13), (14)). Therefore, for bosons we arrive at

$$\begin{aligned} (g_b)^{\beta\beta} (\tilde{n}_b)_\beta &= (\tilde{n}_b)^\beta = \left(\frac{\beta^3 z_b}{2z_b Li_2(z_b) + (z_b - 1) \ln(1 - z_b)^2} \right)^{\frac{1}{2}}, \\ (g_b)^{\beta\gamma_b} (\tilde{n}_b)_\beta &= (\tilde{n}_b)^{\gamma_b} = \frac{(1 - z_b) \ln(1 - z_b)}{z_b} \\ &\quad \times \left(\frac{\beta z_b}{2z_b Li_2(z_b) + (z_b - 1) \ln(1 - z_b)^2} \right)^{\frac{1}{2}}, \end{aligned} \quad (18)$$

and for fermions we have

$$(g_f)^{\beta\beta}(\tilde{n}_f)_\beta = (\tilde{n}_f)^\beta = \left(-\frac{\beta^3 z_f}{2z_f \text{Li}_2(-z_f) + (z_f + 1) \ln(z_f + 1)^2} \right)^{\frac{1}{2}}, \quad (19)$$

$$(g_f)^{\beta\gamma_f}(\tilde{n}_f)_\beta = (\tilde{n}_f)^{\gamma_f} = -\frac{(z_f + 1) \ln(z_f + 1)}{z_f} \times \left(-\frac{\beta z_f}{(1 + z_f) \ln(1 + z_f)^2 + 2z_f \text{Li}_2(-z_f)} \right)^{\frac{1}{2}}.$$

As a result, the extrinsic curvature for bosons takes the following form

$$\begin{aligned} K_b &= \frac{1}{\sqrt{g_b}} \partial_\mu (\sqrt{g_b} n_b^\mu) \\ &= \frac{1}{\sqrt{g_b}} (\partial_\beta (\sqrt{g_b} (\tilde{n}_b)^\beta) + \partial_{\gamma_b} (\sqrt{g_b} (\tilde{n}_b)^{\gamma_b})), \end{aligned} \quad (20)$$

where g_b denotes the determinant of the metric for bosons and $\partial_\mu = (\frac{\partial}{\partial\beta}, \frac{\partial}{\partial\gamma_b})$. The computation for fermions is the same and therefore, the extrinsic curvature for bosons and fermions can be found as follows

$$\begin{aligned} K_b &= \frac{(z_b + \ln(1 - z_b))}{2z_b} \left(\frac{\beta z_b}{2z_b \text{Li}_2(z_b) + (z_b - 1) \ln(1 - z_b)^2} \right)^{\frac{1}{2}}, \\ K_f &= \frac{(z_f - \ln(1 + z_f))}{2z_f} \left(-\frac{\beta z_f}{2z_f \text{Li}_2(-z_f) + (z_f + 1) \ln(1 + z_f)^2} \right)^{\frac{1}{2}}. \end{aligned} \quad (21)$$

Fig.1 and Fig.2 show the extrinsic curvatures of bosons and fermions, respectively, with respect to fugacities z_b and z_f . It is seen that the extrinsic curvature has opposite signs for bosons and fermions. Moreover, There is a singularity for bosons which is located at $z_b = 1$. This point in higher dimensions corresponds to the Bose-Einstein condensation phase transition [7]. It is known that boson gas are less stable than fermion gas [7, 9]. Therefore, we observe the thermodynamic extrinsic curvature of bosons and fermions behaves properly as a geometric tool in study of statistical mechanics of the anyon gas.

Now, let us investigate the extrinsic curvature of anyons. The parameters of space for anyons is (β, γ_a) , where $\gamma_a = -\frac{\mu_a}{k_B T}$. Now, by using Eq.(10), we can replace z_f by $\frac{z_b}{1-z_b}$ in the metric components (Eq.(14)). The unit normal vectors of

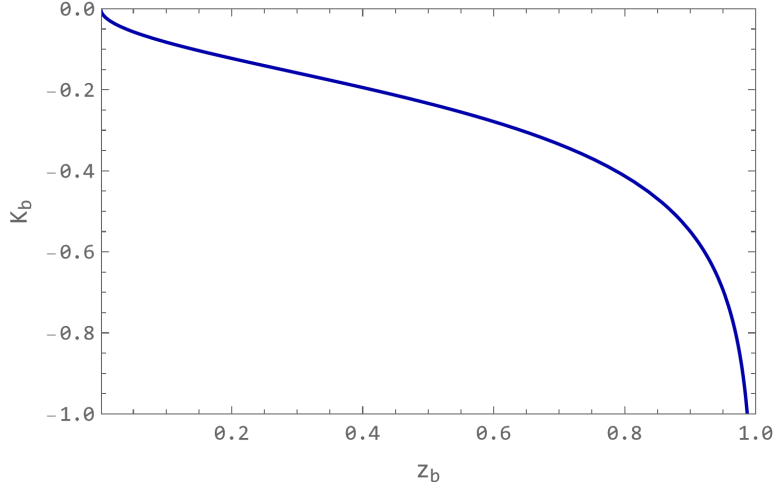


Fig. 1. The thermodynamic extrinsic curvature for bosons as a function of z_b . The singular point at $z_b = 1$ displays Bose-Einstein condensation phase transition. We have set $\beta = 1$.

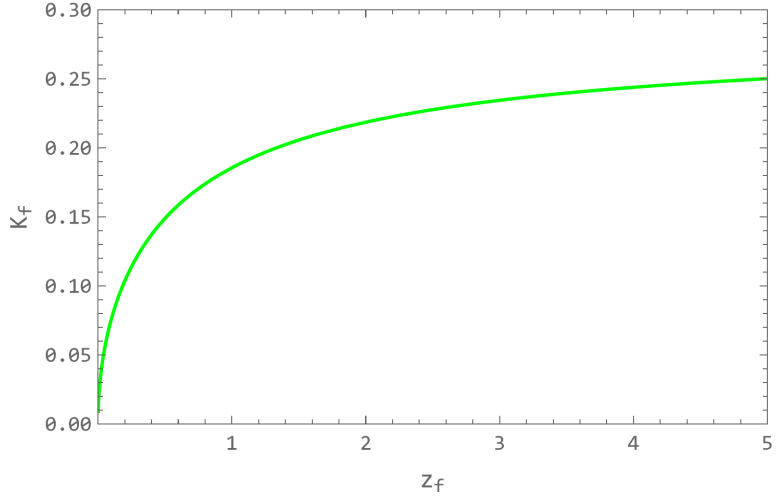


Fig. 2. The thermodynamic extrinsic curvature for fermions as a function of z_f and $\beta = 1$.

anyons with upper indicies take the following form

$$\begin{aligned}
 (\tilde{n}_a)^\beta &= \left(\frac{\beta^3 z_b}{2(1-\alpha)z_b \operatorname{Li}_2(z_b) - 2\alpha z_b \operatorname{Li}_2\left(\frac{z_b}{z_b-1}\right) + ((1-\alpha)z_b - 1)\left(\alpha \ln\left(\frac{1}{1-z_b}\right) - (1-\alpha)\ln(1-z_b)\right)^2} \right)^{\frac{1}{2}}, \\
 (\tilde{n}_a)^{\gamma_a} &= \frac{((1-\alpha)z_b - 1)\left(\alpha \ln\left(\frac{1}{1-z_b}\right) + (\alpha-1)\ln(1-z_b)\right)}{z_b} \\
 &\quad \times \left(\frac{\beta z_b}{2(1-\alpha)z_b \operatorname{Li}_2(z_b) - 2\alpha z_b \operatorname{Li}_2\left(\frac{z_b}{z_b-1}\right) + ((1-\alpha)z_b - 1)\left(\alpha \ln\left(\frac{1}{1-z_b}\right) + (\alpha-1)\ln(1-z_b)\right)^2} \right)^{\frac{1}{2}}.
 \end{aligned}
 \tag{22}$$

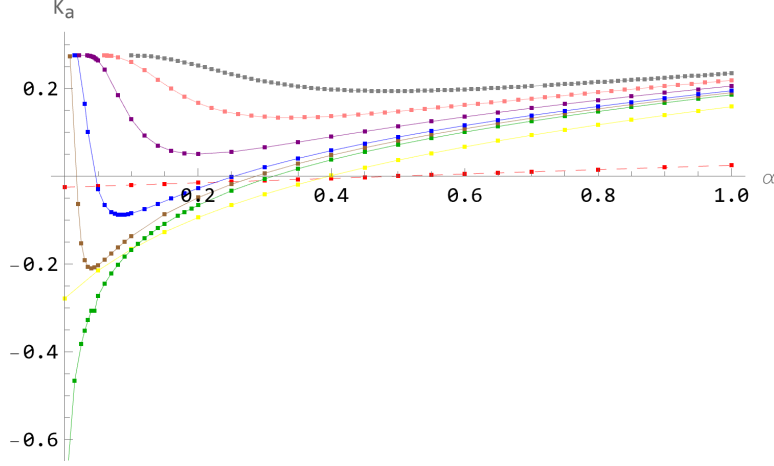


Fig. 3. The thermodynamic extrinsic curvature of anyon gas as a function of α . The values of anyon fugacity have been considered as $z_a = 0.01$ (dashed red curve), 0.6 (yellow curve), 1.0 (green curve), 1.1 (brown), 1.2 (blue), 1.5 (purple), 2.0 (pink) and 3.0 (gray upper curve). We have set $\beta = 1$ for all diagrams.

The extrinsic curvature of anyons is given by

$$K_a = \frac{1}{\sqrt{g_a}} \left(\partial_\beta (\sqrt{g_a} (\tilde{n}_a)^\beta) + \partial_{\gamma_a} (\sqrt{g_a} (\tilde{n}_a)^{\gamma_a}) \right), \quad (23)$$

where g_a denotes the determinant of the metric of anyons which components are given in Eq.(14). Eq.(9) implies $\gamma_a = \alpha \gamma_f + (1 - \alpha) \gamma_b$, therefore we can write the second term in Eq.(23) as follows

$$\begin{aligned} \partial_{\gamma_a} (\sqrt{g_a} (\tilde{n}_a)^{\gamma_a}) &= \frac{1}{\frac{\partial \gamma_a}{\partial (\sqrt{g_a} (\tilde{n}_a)^{\gamma_a})}} \\ &= \left(\frac{\alpha}{\partial \gamma_f (\sqrt{g_a} (\tilde{n}_a)^{\gamma_a})} + \frac{(1 - \alpha)}{\partial \gamma_b (\sqrt{g_a} (\tilde{n}_a)^{\gamma_a})} \right)^{-1} \\ &= \left(\frac{\alpha (1 + \frac{z_b}{1 - z_b})}{\partial \gamma_b (\sqrt{g_a} (\tilde{n}_a)^{\gamma_a})} + \frac{(1 - \alpha)}{\partial \gamma_b (\sqrt{g_a} (\tilde{n}_a)^{\gamma_a})} \right)^{-1}, \end{aligned} \quad (24)$$

where we have used Eq.(10), $\frac{\partial}{\partial \gamma_f} = \frac{\partial \gamma_b}{\partial \gamma_f} \frac{\partial}{\partial \gamma_b}$ and $\frac{\partial \gamma_b}{\partial \gamma_f} = (1 + \frac{z_b}{1 - z_b})^{-1}$. Fig.3 shows the extrinsic curvature for different values of anyon fugacities. In the classical limit we have obtained Eq.(15) therefore at $\alpha = \frac{1}{2}$ it represents a classical ideal gas ($PV = Nk_B T$). It is seen for $z_a = 0.01$ the extrinsic curvature behaves as an ideal classical gas whose sign changes at $\alpha = \frac{1}{2}$. For larger values of z_a , we observe a fermionic behavior where the extrinsic curvature is positive. The extrinsic curvature has a minimum point for $z_a > 1$ that exists in the range $\alpha < \frac{1}{2}$. As the value of anyon fugacity increases the minimum point goes toward the bigger values of α . Furthermore, for some values of anyon fugacities ($z_a > 1$), there are two points of

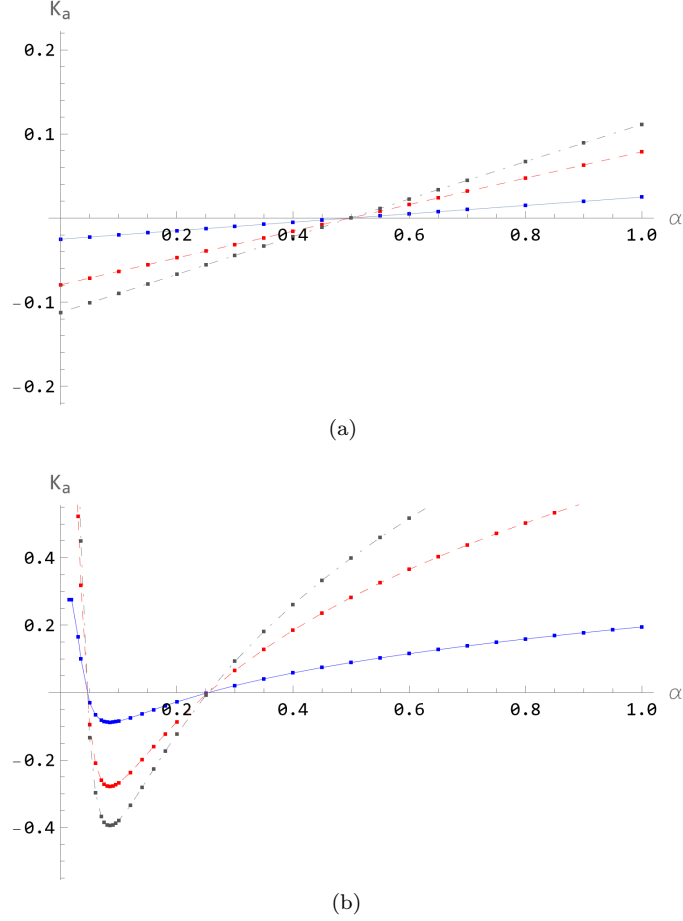


Fig. 4. The thermodynamic extrinsic curvature of anyon gas as a function of α for different β hypersurfaces. The diagrams are for $\beta = 20$ (dotted-dashed gray curve), $\beta = 10$ (dashed-red curve) and $\beta = 1$ (solid blue curve) at constant anyon fugacities (a) $z_a = 0.01$ (b) $z_a = 1.2$.

α where the extrinsic curvature has the same amount, indicating a duality relation between those points. For $z_a = 1$, the extrinsic curvature goes to negative infinity (green curve) at $\alpha = 0$ that represents the bosonic behavior. The results are in agreement with behavior of thermodynamic Ricci scalar that was investigated in [9].

Now, let us investigate the thermodynamic extrinsic curvature for different values of β hypersurfaces. Fig.4 shows the thermodynamic extrinsic curvature as a function of α for three values of inverse temperatures β . First, we consider the classical limit and $z_a = 0.01$. There is a fixed point that the value of the thermodynamic extrinsic curvature is equal to zero for all values of inverse temperatures, where $\alpha = 0.5$ in Fig.4(a). At this fixed point, the gas particles behave as semions

and do not have bosonic or fermionic behavior. Then, we restrict our attention to the other interesting case $z_a = 1.2$. Fig.4(b) shows by increasing the value of inverse temperature β (upper curves to downer curves) the minimum absolute value of the extrinsic curvature increases which moves toward the small values of α . Therefore, for larger values of β or as $T \rightarrow 0$, the thermodynamic extrinsic curvature for $\alpha = 0$ has the bosonic behavior with $K_a < 0$. Also, we observe semionic behavior of the anyon gas particles where $\alpha = 0.25$. Therefore, for values away from the classical limit, the fixed point with $K_a = 0$ moves toward the small values of α . Also, we find two different points with $K_a = 0$. These new fixed points can not be obtained by using the thermodynamic Ricci scalar curvature.

4. Critical systems

Thermodynamic geometry of the two dimensional Kagome Ising model was investigated in [11]. It was shown that at zero magnetic field the thermodynamic scalar curvature behaves as $R \sim \varepsilon^{\alpha-1}$ where $\varepsilon = \beta - \beta_c$ and $\alpha = 0$ (β_c denotes the critical point). For positive values of α the critical behavior of the thermodynamic scalar curvature is $R \sim \varepsilon^{\alpha-2}$ [15]. The critical scaling behavior of the thermodynamic scalar curvature not only determines the phase transition points but also can be used to extract the critical exponent α . Consider the critical region, where we expect a standard scaling form of the free energy per site as follows

$$f(\varepsilon, h) = \lambda^{-1} f(\varepsilon \lambda^{a_\varepsilon}, h \lambda^{a_h}), \quad (25)$$

where a_h and a_ε are scaling dimensions of spin operators and the energy, respectively. In the high temperature region ($\varepsilon = \beta_c - \beta > 0$), using the scaling assumptions and the scaling function ψ_+ we arrive at

$$f(\varepsilon, h) = \varepsilon^{\frac{1}{a_\varepsilon}} \psi_+(h \varepsilon^{-\frac{a_h}{a_\varepsilon}}). \quad (26)$$

In the second order transition, the scalar curvature can be written as $R \sim \xi^d$, where d is the dimension of the system and ξ is the correlation length. Here, we are going to obtain the critical exponents via the scaling behavior of the extrinsic curvature. We study the two dimensional Kagome Ising model and the spherical model. The relevant parameters of the spin systems are (β, h) where $\beta = \frac{1}{k_B T}$ and h is the external magnetic field.

4.1. Kagome Ising model

The two dimensional Ising model in a magnetic field background has been studied by different methods [38, 39]. Fisher obtained a unique exact solution of an anti-ferromagnetic Ising model [40]. The Fisher model was defined on a square lattice in the nonzero magnetic field. It was also generalized to the Ising model on the Kagome lattice and in a magnetic field background which is soluble for a few cases [41–44]. In one of the cases, the Kagome Ising model was solved by using the equivalency between those partition functions of the Kagome and the Honeycomb Ising

models [44]. That case transforms into the Fisher model for the square lattice. In recent years, Kagome lattice has received attention for its applications in high-Tc superconductivity. Here, we obtain the thermodynamic extrinsic curvature and the critical exponent using the Fisher model. For an Ising model on the Kagome lattice, see Fig.5, the interacting energy of every triangle composed of the spins $\sigma_1, \sigma_2, \sigma_3$ is given by

$$-J_1\sigma_1\sigma_2 + J(\sigma_2\sigma_3 - \sigma_3\sigma_1) - \mu H(\sigma_1 + \sigma_2), \quad (27)$$

where H denotes the magnetic field which affects the $\frac{2}{3}$ of sites on the lattice. The reduced field determines by $h = \beta H$ and reduce interactions are $b = \beta J, b_1 = \beta J_1$. The Ising spin σ_3 with zero magnetic moment does not couple to the magnetic field. Therefore, σ_1, σ_2 have a super-exchange interaction with the spin σ_3 (non-magnetic). The Fisher model can be obtained from this model by assuming $b_1 = 0$. The partition functions of the Ising model on the kagome and Honeycomb lattices are equivalent at zero magnetic field, $Z_{KG} = F^N Z_{HC}$, where N represents the number of lattice sites in the Honeycomb model and the magnetic spins in the Kagome lattice, the parameter F is a constant. The per-site free energy for Honeycomb lattice and the per magnetic spin free energy are, respectively, given by

$$f_{HC} = \lim_{N \rightarrow \infty} N^{-1} \ln Z_{HC}, \quad \text{and} \quad f_{KG} = \lim_{N \rightarrow \infty} N^{-1} \ln Z_{KG}, \quad (28)$$

The relation of F_{HC} was reported in [45, 46]. Therefore, by using Eq.(28) we arrive at the free energy of Kagome Ising model

$$f = \frac{1}{16\pi^2} \int_0^{2\pi} \int_0^{2\pi} d\theta d\varphi \xi(\theta, \varphi) + \frac{3}{4} \ln 2 + \ln F, \quad (29)$$

where

$$\begin{aligned} \xi(\theta, \varphi) &= \cosh 2r_1 \cosh^2 2r - \sinh^2 2r \cos(\theta + \varphi) - \sinh 2r_1 \\ &\quad \times \sinh 2r(\cos \theta + \cos \varphi) + 1, \end{aligned} \quad (30)$$

and r_1 and r are, respectively, as a function of b_1 and b . We have the Fisher model in the case $b_1 = 0$. Therefore, by Setting $b_1 = 0$ in the above relation, we can write the free energy per spin as follows [44]

$$f = f_1(b, h) + f_2(r), \quad (31)$$

where $f_1(b, h), f_2(r)$ are defined as follows

$$f_1(b, h) = \frac{1}{4} \ln \{ \cosh^2 h (\sinh^2 h + \cosh^2 2b) \} + \frac{3}{2} \ln 2, \quad (32)$$

$$f_2(r) = \frac{1}{16\pi^2} \int_0^{2\pi} \int_0^{2\pi} d\theta d\varphi \ln \{ \cosh^2 2r - \sinh 2r (\cos \theta + \cos \varphi) \}.$$

Also, r fulfills the below relation

$$r = -\frac{1}{4} \ln \left(\frac{\sinh^2 h + \cosh^2 2b}{\cosh^2 h} \right). \quad (33)$$

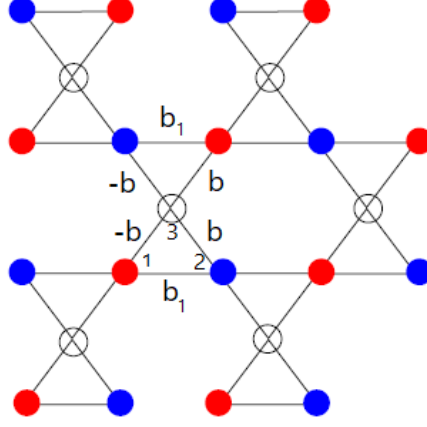


Fig. 5. Kagome Ising lattice in a magnetic field. Colorful circles show magnetic Ising spins 1, 2 and open circles non-magnetic spins 3.

With some simplifications $f_2(r)$ takes the following form [11]

$$f_2(r) = \frac{1}{\pi} \int_0^{\frac{\pi}{2}} d\theta \ln\left(\frac{1}{2}(1 + \sqrt{1 - \kappa^2 \sin^2 \theta})\right) + \frac{1}{2} \ln(\cosh^2 2r), \quad (34)$$

where $\kappa = -\frac{2 \sinh 2r}{\cosh^2 2r}$. Here, the parameters of the thermodynamic space are (b, h) and from the metric defined in Eq.(1) where $\ln Z = f$, the metric elements of two dimensional Kagome Ising model are given by

$$g_{ij} \equiv f_{ij} = \partial_i \partial_j f. \quad (35)$$

Therefore, we arrive at

$$\begin{aligned} g_{bb} &\equiv f_{bb} = \frac{\partial f_b}{\partial b}, \\ g_{hh} &\equiv f_{hh} = \frac{\partial f_h}{\partial h}, \\ g_{hb} &= g_{bh} \equiv f_{bh} = \frac{\partial f_h}{\partial b}, \end{aligned} \quad (36)$$

where

$$\begin{aligned} f_b &\equiv \frac{\partial f}{\partial b} = \frac{\partial f_1}{\partial b} + \frac{\partial f_2}{\partial r} \frac{\partial r}{\partial b}, \\ f_h &\equiv \frac{\partial f}{\partial h} = \frac{\partial f_1}{\partial h} + \frac{\partial f_2}{\partial r} \frac{\partial r}{\partial h}. \end{aligned} \quad (37)$$

The relations are lengthy so we write them in the general form. The first derivatives of free energy can be found in Appendix. The thermodynamic geometry of

the Kagome Ising model in two dimensions was studied in [11]. The results show the scalar curvature R is positive at high temperature that shows disordered state (paramagnetic), while it is negative for low temperature ordered state (antiferromagnetic). Moreover, as the temperature decreases the scalar curvature diverges at plus infinity. It was shown the critical line where the scalar curvature also diverges at the same points coincides with the Fisher expression

$$h = \operatorname{arccosh} \left(\sqrt{\frac{\sqrt{2}-1}{2}} \sinh(2b) \right), \quad (38)$$

and in the zero field case ($h = 0$) upon setting the denominator of R equals to zero, the critical point is obtained as

$$b_c = \operatorname{arccosh} \left(\sqrt{\frac{2+\sqrt{2}}{2}} \right), \quad (39)$$

where b_c denotes the critical point. Now, we will obtain the extrinsic curvature using the Fisher model. We first assume a constant b hypersurface, therefore from Eq.(4) we have $\tilde{n}_b = \frac{\partial_b \mathcal{H}}{\sqrt{g^{bb} \partial_b \mathcal{H} \partial_b \mathcal{H}}}$. From this relation, the upper indices unit normal vectors for constant b hypersurface takes the following form

$$\begin{aligned} \tilde{n}^b &= g^{bb} \tilde{n}_b = \frac{f^{bb}}{\sqrt{f^{bb}}}, \\ \tilde{n}^h &= g^{bh} \tilde{n}_b = \frac{f^{bh}}{\sqrt{f^{bb}}}, \end{aligned} \quad (40)$$

where we have used Eq.(36). Then, by making use of Eq.(3) the extrinsic curvature is expressed as

$$K = \frac{1}{\sqrt{g}} (\partial_b (\sqrt{g} \tilde{n}^b) + \partial_h (\sqrt{g} \tilde{n}^h)), \quad (41)$$

where g denotes the determinant of the two dimensional Kagome Ising metric. Also, the computation of the thermodynamic extrinsic curvature for the h constant hypersurface can be done by using the following unit normal vectors ($\tilde{n}_h = \frac{1}{\sqrt{g^{hh}}}$)

$$\begin{aligned} \tilde{n}^b &= g^{bb} \tilde{n}_h = \frac{f^{bb}}{\sqrt{f^{hh}}}, \\ \tilde{n}^h &= g^{bh} \tilde{n}_h = \frac{f^{bh}}{\sqrt{f^{hh}}}. \end{aligned} \quad (42)$$

We have depicted the thermodynamic extrinsic curvature of the 2-d Kagome Ising model in Fig.6 and Fig.7, respectively, for different h and b hypersurfaces. The points $h = 1.24$ and $b = 1.06$ satisfy the Fisher expression in Eq.(38). Fig.6 and Fig.7 show divergence points of the thermodynamic extrinsic curvature, properly. The divergence points correspond to the phase transition points. Moreover, Fig.6 shows that $K < 0$ at high temperature or small value of β while $K > 0$ for low

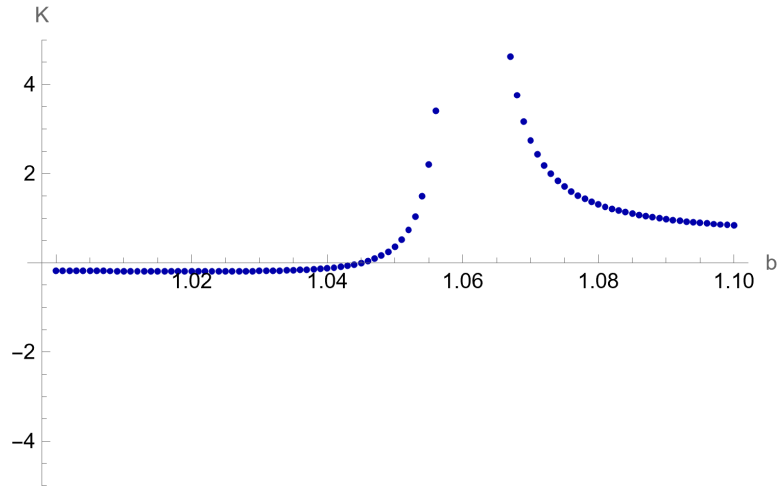


Fig. 6. Thermodynamic extrinsic curvature K of two dimensional Kagome Ising model for h hypersurface. At $h = 1.24$, the thermodynamic extrinsic curvature K diverges at the critical point $b = 1.06$.

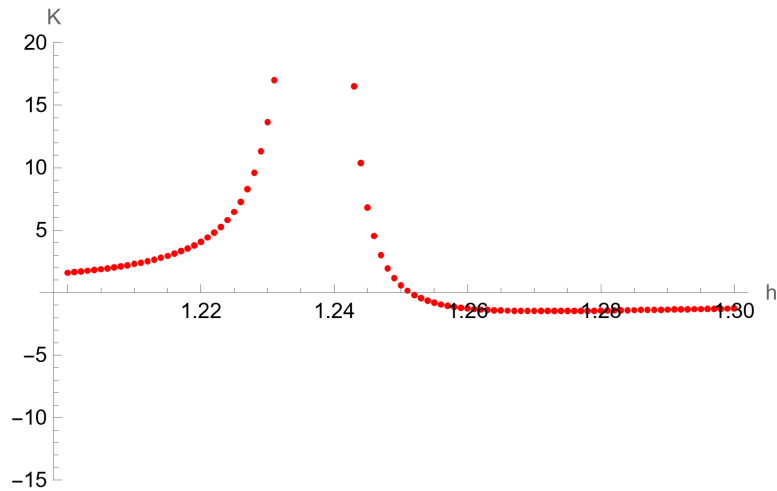


Fig. 7. Thermodynamic extrinsic curvature K of two dimensional Kagome Ising model for b hypersurface. At $b = 1.06$, K diverges at the critical point $h = 1.24$.

temperature. Therefore, by decreasing the temperature a transition occurs from the disordered (paramagnetic) to an ordered state (antiferromagnetic). In Fig.7, by increasing an external field we observe a phase transition from the ordered state ($K > 0$) to the disordered state ($K < 0$) at the critical point $h_c = 1.24$. We also observe that signs of the thermodynamic extrinsic curvature K and the thermodynamic scalar curvature are opposite to each other. The thermodynamic extrinsic

curvature is depicted at zero magnetic field in Fig.8. It is seen that the divergence point corresponds to the critical point in Eq.(39) exactly. The correspondence of the divergence points of the thermodynamic extrinsic and scalar curvatures is an important issue that should be studied more in the future.

Now, we are going to derive the critical behavior of the thermodynamic extrinsic curvature. As usual, we expect a power law behavior near critical points. Therefore, around the critical points, the extrinsic curvature behaves as $K \propto -(1 - \tilde{b}_+)^a$ or

$$\ln |K| = -a \ln (1 - \tilde{b}_+) + c, \quad (43)$$

where the reduced parameter $\tilde{b}_+ = \frac{b}{b_c}$ and b_c is the critical point, where K diverges. In the following lines, we obtain the scaling behavior of the extrinsic curvature at zero magnetic field, $h = 0$ hypersurface. Using the definition of the extrinsic curvature in Eq.(41), we can compute Eq.(43) for different values of b near the critical point b_c (Eq.(39)). We extrapolate the numerical values and find the coefficients a and c by a numerical method. We indicate the numerical results in Fig.9 by blue points and the red fitting line. From Fig.9 we obtain $a \simeq 0.07148$ and $c \simeq 1.75139$. Extrapolating the numerical values, our results are consistent with $a = 0$. So, we find that the thermodynamic extrinsic curvature behaves as $K \sim (b - b_c)^\alpha \equiv \varepsilon^\alpha$, where $\alpha = 0$ as it was expected. However, it was found that the thermodynamic scaling behavior of the scalar curvature is $R \sim \varepsilon^{\alpha-1}$ with $\alpha = 0$ which is the same as 2d-Ising model on planar random graph with $\alpha = -1$. There is a unit of difference between the power of the thermodynamic scalar and extrinsic curvatures. Also, we have recently studied thermodynamic of pure Lovelock black holes by using thermodynamic geometry method [47]. We have found the scaling behavior of the scalar and the extrinsic curvatures are, respectively, $R \sim \varepsilon^{\alpha-2}$ and $K \sim \varepsilon^{\alpha-1}$ with $\alpha = 0$. It is interesting that a universal behavior appears as $\frac{R}{K} \sim \frac{1}{\varepsilon}$ for different models such as pure Lovelock black holes and Kagome Ising model.

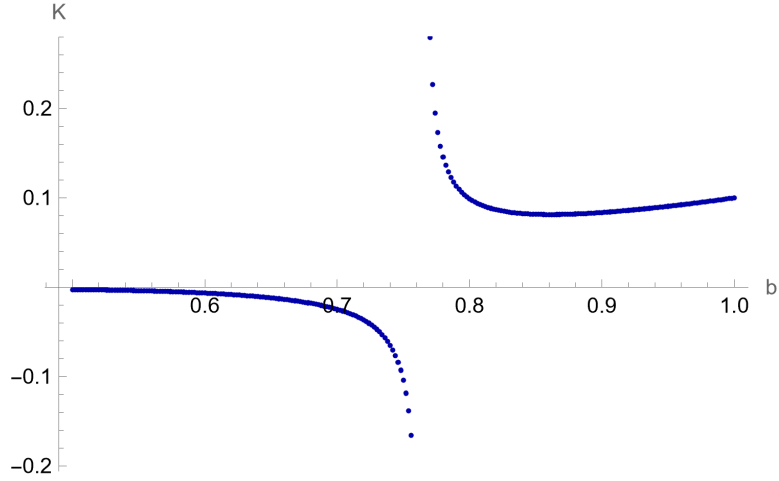


Fig. 8. Extrinsic curvature of two dimensional Kagome Ising model at $h = 0$ hypersurface, the critical point is $b_c = 0.76$.

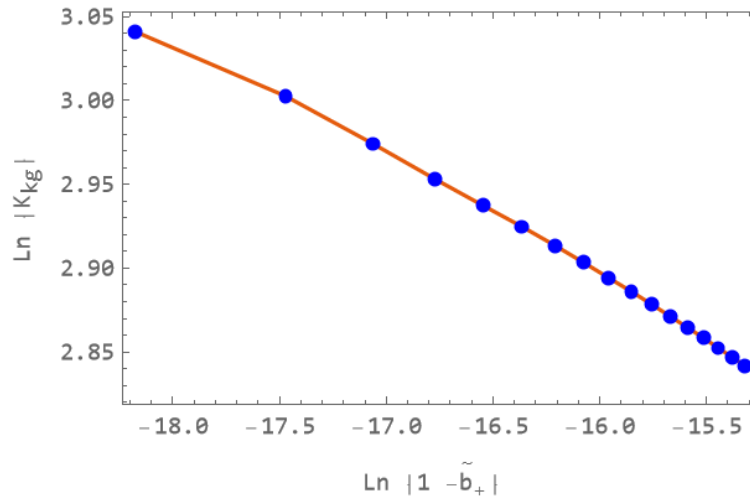


Fig. 9. The numerical values (blue points) of $\ln |K_{kg}|$ as a function of $\ln(1 - \tilde{b}_+)$ for two dimensional Kagome Ising model near the critical point $b_c = 0.76428$. The data are fitted by the red line with the slope 0.07148.

4.2. The spherical model

The spherical model is a generalized form of the two dimensional Ising model. Kac introduced this model that spin variable s_i have arbitrary values [48] such as

$$\sum_i s_i^2 = N. \quad (44)$$

Therefore, the value of the spin can vary continuously on the sphere with the radius $N^{\frac{1}{2}}$ from $-N^{\frac{1}{2}}$ to $N^{\frac{1}{2}}$. This approach is useful for spin models with an external field. In 1952, Berlin and Kac solved this model for one, two and three dimensions. Three dimensional spherical model presents transition at finite temperature while one and two dimensional cases do not that differs from the two dimensional Ising model. The model is reliable for entire temperatures. It was shown that the critical exponents of the Ising model on two dimensional planar random graphs are the same as the three dimensional spherical model [49, 50] and $\alpha = -1$. As α is negative the scalar curvature behaves as $R \sim \varepsilon^{\alpha-1}$ rather than $R \sim \varepsilon^{\alpha-2}$. Moreover, for $d \geq 4$ the model can be described by a mean field theory with $\alpha = 0$. The spherical model's partition function is given by

$$Z = \int ds_1 \dots ds_N \exp(\beta \sum_{\langle ij \rangle} s_i s_j + h \sum_i s_i) \delta(\sum_i s_i^2 - N), \quad (45)$$

where s_i denotes the value of a spin, N is the number of sites and h is the magnetic field. Using the saddle-point method and $f = \ln Z$, the free energy in the thermodynamic limit ($N \rightarrow \infty$) is written as

$$f = \frac{1}{2} \text{Log} \left(\frac{\pi}{\beta} \right) + \beta z - \frac{1}{2} g(z) + \frac{h^2}{4\beta(z-d)}, \quad (46)$$

where

$$g(z) = \frac{1}{(2\pi)^d} \int_0^{2\pi} d\omega_1 \dots d\omega_d \text{Log} \left(z - \sum_{k=1}^d \cos(\omega_k) \right). \quad (47)$$

Therefore, the saddle point for the free energy is given by

$$g'(z) = 2\beta - \frac{h^2}{2\beta(z-d)^2}. \quad (48)$$

We focus our attention to the case $d = 3$, since there is no phase transition for $d = 1$ and $d = 2$. Using Eq.(48) with $h = 0$ we have

$$\frac{dz}{d\beta} = \frac{2}{g''(z)}, \quad (49)$$

therefore

$$\frac{d^2 z}{d\beta^2} = \frac{-4g'''(z)}{g''(z)^3}. \quad (50)$$

The critical point is given by $z = d = 3$ for $h = 0$ and the phase transition correlate with the spontaneous magnetization in three dimensional lattice [48]. To reach $g(z)$ in the critical region, we derive the second derivative of $g(z)$ by differentiating Eq.(47) and expanding around small values of ω_k therefore we have

$$g''(z) \sim \frac{-1}{2\sqrt{2}\pi} (z-3)^{-\frac{1}{2}}, \quad (51)$$

20

and

$$g'''(z) \sim \frac{1}{4\sqrt{2\pi}}(z-3)^{-\frac{3}{2}}. \quad (52)$$

Therefore by integrating we have

$$g'(z) \sim \frac{1}{4\sqrt{2\pi}}(z-3)^{\frac{1}{2}} + g'(3), \quad (53)$$

Now, inserting $h = 0$ in Eq.(48) and using the above relation we arrive at the following relation

$$(z-3) \sim 8\pi^2(\beta - \beta_c)^2 \sim \varepsilon^2, \quad (54)$$

where $\beta_c = \frac{g'(3)}{2} \approx 0.25$. Therefore by using Eq.(51) and Eq.(52), the scaling behavior of $\frac{dz}{d\beta}$ and $\frac{d^2z}{d\beta^2}$ from Eq.(49) and Eq.(50) may be written as

$$\lim_{z \rightarrow 3} \frac{dz}{d\beta} = \lim_{z \rightarrow 3} \left\{ -4\sqrt{2\pi}(z-3)^{\frac{1}{2}} \right\} = 0, \quad (55)$$

$$\lim_{z \rightarrow 3} \frac{d^2z}{d\beta^2} = 16\pi^2. \quad (56)$$

It was shown that for $\alpha = -1$ the scalar scalar curvature behaves as $R \sim \varepsilon^{\alpha-1}$ [51]. We expect that this type of scaling behavior of R to be universal for $\alpha < 0$. In the next section, we derive the scaling behavior of the thermodynamic extrinsic curvature by a simple method.

5. The critical behavior of the extrinsic curvature

In this section, we derive the scaling form of the extrinsic curvature by using Eq.(26). We also simplify the notation and define $A = \frac{1}{a_\varepsilon}$, $C = \frac{-a_h}{a_\varepsilon}$. With respect to standard critical exponents we have $A = 2 - \alpha$ and $A + C = \beta$ [51]. Therefore, from Eq.(26) the scaling form of the free energy is given by $f = \varepsilon^A \psi_+(h \varepsilon^C)$, where $\varepsilon = \beta_c - \beta$ and h is the external magnetic field. The scaling form of the metric elements with parameters (β, h) are calculated in the following form

$$\begin{aligned} g_{\beta\beta} &= \partial_\beta^2 f = A(A-1)\phi(0), \\ g_{hh} &= \partial_h^2 f = \varepsilon^{A+2C} \psi_+''(h \varepsilon^C), \\ g_{\beta h} &= g_{h\beta} = \partial_\beta \partial_h f = -\varepsilon^{A+C-1} \left((A+C) \psi_+'(h \varepsilon^C) + C h \varepsilon^C \psi_+''(h \varepsilon^C) \right), \end{aligned} \quad (57)$$

which is for $\alpha < 0$ ($A > 2$). In this case, we expect that the specific heat is a constant at the critical point and we define it by $A(A-1)\phi(0)$, where $\phi(0)$ is a constant function. We assume a constant β hypersurface. Using Eq.(4), the unit normal vector is given by

$$\begin{aligned} \tilde{n}_\beta &= \frac{1}{\sqrt{g^{\beta\beta}}} \\ &= \left(\frac{A(A-1)\phi(0)\psi_+''(h \varepsilon^C) - \varepsilon^{A-2} \left((A+C)\psi_+'(h \varepsilon^C) + C h \varepsilon^C \psi_+''(h \varepsilon^C) \right)^2}{\psi_+''(h \varepsilon^C)} \right)^{\frac{1}{2}}. \end{aligned} \quad (58)$$

Table 1. The standard scaling behavior of the thermodynamic scalar and extrinsic curvatures for the spherical model at the critical point ($h = 0$), where, $\alpha < 0$ and $\alpha > 0$ are, respectively, for $d = 3$ and $d = 4$. Derivation of the scaling thermodynamic extrinsic curvature was done on an isotherm hypersurface.

Extrinsic curvature	Scalar curvature	α
$K \sim \varepsilon^\alpha$	$R \sim \varepsilon^{\alpha-1}$	$\alpha < 0$
$K \sim \varepsilon^{\frac{1}{2}(\alpha-2)}$	$R \sim \varepsilon^{\alpha-2}$	$\alpha > 0$

The upper indices of the vector are given by

$$\begin{aligned}\tilde{n}^\beta &= g^{\beta\beta} \tilde{n}_\beta = \frac{g^{\beta\beta}}{\sqrt{g^{\beta\beta}}}, \\ \tilde{n}^h &= g^{\beta h} \tilde{n}_\beta = \frac{g^{\beta h}}{\sqrt{g^{\beta\beta}}}.\end{aligned}\tag{59}$$

Then the extrinsic curvature by using Eq.(3) at zero magnetic field ($h = 0$) near the critical point ($\varepsilon \rightarrow 0$) is written in the following form

$$\begin{aligned}K &= \frac{1}{\sqrt{g}} (\partial_\beta(\sqrt{g} \tilde{n}^\beta) + \partial_h(\sqrt{g} \tilde{n}^h)) \\ &= \frac{\varepsilon (\psi_+'''(0) (A + C) \psi_+'(0) - (A + 2C) \psi_+''(0)^2) \left((A - 1)A \phi(0) - \frac{(A+C)^2 \psi_+'(0)^2 \varepsilon^{A-2}}{\psi_+'(0)} \right)^{\frac{1}{2}}}{2\psi_+''(0) ((A - 1)A \phi(0) \varepsilon^2 \psi_+''(0) - (A + C)^2 \psi_+'(0)^2 \varepsilon^A)} \\ &= -\frac{A + 2C}{2\varepsilon(A(A - 1)\phi(0))^{\frac{1}{2}}},\end{aligned}\tag{60}$$

where, g denotes the determinant of the metric in Eq.(57). We have used $\psi'(0) = 0$ and $\psi'''(0) = 0$ since the odd h derivatives of the scaling function should vanish at $h = 0$ for Ising-like models [52]. Therefore in the case $\alpha < 0$, we find the scaling behavior of the extrinsic curvature is $K \sim \varepsilon^{-1}$ which is consistent with $K \sim \varepsilon^\alpha$, where $\alpha = -1$. However, the scaling behavior of the thermodynamic scalar curvature can be obtained as $R \sim \varepsilon^{\alpha-1}$ for $\alpha < 0$ which is the same as the two dimensional Ising model on planar random graph. This result is in accordance with the standard scaling behavior of the thermodynamic scalar curvature for negative α . Therefore we expect that the extrinsic curvature of three dimensional spherical model behaves as $K \sim \varepsilon^\alpha$.

The spherical model has mean field behavior in $d \geq 4$ with $\alpha = 0$. The scaling behavior of the thermodynamic scalar curvature is $R \sim \varepsilon^{-2}$ which corresponds to $R \sim \varepsilon^{\alpha-2}$, where $\alpha = 0$. In this case, the scaling metric elements are given by

$$\begin{aligned}g_{\beta\beta} &= \partial_\beta^2 f, \\ g_{hh} &= \partial_h^2 f = \varepsilon^{A+2C} \psi_+''(h \varepsilon^C), \\ g_{\beta h} &= g_{h\beta} = \partial_\beta \partial_h f = -\varepsilon^{A+C-1} ((A + C) \psi_+'(h \varepsilon^C) + C h \varepsilon^C \psi_+''(h \varepsilon^C)),\end{aligned}\tag{61}$$

where $f = \varepsilon^A \psi_+(h \varepsilon^C)$ as before. Therefore, $g_{\beta\beta}$ in Eq.(61) is not constant and is given by $A(A-1)\varepsilon^{A-2} \psi_+(0)$ at $h=0$ which is different from $g_{\beta\beta}$ in Eq.(57). The normal vector components indices \tilde{n}_β , \tilde{n}^β and \tilde{n}^h can be obtained as before. We derive the standard scaling behavior of the thermodynamic extrinsic curvature at zero magnetic field ($h=0$) near the critical point ($\varepsilon \rightarrow 0$) as follows

$$\begin{aligned} K &= \frac{1}{\sqrt{g}} (\partial_\beta(\sqrt{g} \tilde{n}^\beta) + \partial_h(\sqrt{g} \tilde{n}^h)) \\ &= \frac{((A+C)\psi'_+(0)\psi''_+(0) - (A+2C)\psi''_+(0)^2) \left(\frac{\psi''_+(0)\varepsilon^{2-A}}{(A-1)A\psi_+(0)\psi''_+(0) - (A+C)^2\psi'_+(0)^2} \right)^{\frac{1}{2}}}{2\varepsilon\psi''_+(0)^2} \\ &= -(A+2C) \left(\frac{\varepsilon^{-A}}{(A-1)A\psi_+(0)} \right)^{\frac{1}{2}}, \end{aligned} \quad (62)$$

where we have used $\psi'(0) = 0$ and $\psi'''(0) = 0$. Therefore, we expect that the scaling behavior of the thermodynamic extrinsic curvature of the spherical model behaves as $K \sim \varepsilon^{\frac{1}{2}(\alpha-2)}$ for $d \geq 4$ while the scaling behavior of the scalar curvature is $R \sim \varepsilon^{\alpha-2}$, where $\alpha = 0$. It should be noted that we obtain the same scaling behavior of the thermodynamic extrinsic curvature by assuming a constant h hypersurface. Moreover, we expect that the same behavior to be valid for $\alpha > 0$ in $d \geq 4$, we have gathered the whole results in Table 1.

6. Conclusions

The thermodynamic extrinsic curvature is a geometric tool for observing some aspects of statistical mechanics. It is a new geometric window to observe the critical phenomena. In this paper, we investigated the thermodynamic extrinsic curvature of an anyon gas. We explored nonperturbative thermodynamic extrinsic curvature of an anyon gas K_a at constant fugacities $z_a = 0.01$ and $z_a = 1.2$ and obtained certain fixed points that particles behave as semions. This is a new result that can not be obtained in the context of the thermodynamic Ricci scalar curvature. Then, we studied the two dimensional Kagome Ising model and showed that $K \sim \varepsilon^\alpha$ with $\alpha = 0$. Therefore, for two dimensional Ising models with $\alpha \leq 0$ we expect that the scaling of the extrinsic curvatures behave as $K \sim \varepsilon^\alpha$. Then, we derived the scaling behavior of the extrinsic curvature related to the spherical model. We found that the scaling extrinsic curvature behaves as $K \sim \varepsilon^\alpha$ with $\alpha = -1$. We also studied the spherical model in $d \geq 4$ and obtained $K \sim \varepsilon^{\frac{1}{2}(\alpha-2)}$, where $\alpha = 0$. However, for $\alpha > 0$ we derived a different scaling behavior for the extrinsic curvature as $K \sim \varepsilon^{\frac{1}{2}(\alpha-2)}$. In this work, we obtained some important properties of the extrinsic curvature. The fermion gas and an ordered state of the two dimensional Kagome Ising model have positive thermodynamic extrinsic curvatures. It should be noted that the sign of the thermodynamic extrinsic curvature is positive for stable states. Also, we showed the results from the computing thermodynamic extrinsic curvature of Kagome Ising model $K \sim \varepsilon^\alpha$ is consistent with what we expected from

the standard scaling behavior of the thermodynamic extrinsic curvature. We hope to study the extrinsic curvature and related geometric pictures for other physical systems in the near future.

Acknowledgments

We would like to thank Isfahan University of Technology for financial support.

Appendix

Usefull equations that are related to Eq.(37):

$$\frac{\partial f_1}{\partial b} = \frac{\sinh 2b \cosh 2b}{\sinh^2 h + \cosh^2 2b}, \quad \frac{\partial f_1}{\partial h} = \frac{\tanh h (\cosh^2 2b + \cosh^2 h)}{\cosh 4b + \cosh 2h}, \quad (\text{A.1})$$

and

$$\begin{aligned} \frac{\partial f_2}{\partial b} &= \frac{1}{16\pi(\cosh 4b + \cosh 2h)^2} \operatorname{csch} \left[\frac{1}{2} \log(\cosh^2 2b \operatorname{sech}^2 h + \tanh^2 h) \right] \\ &\times \operatorname{sech} \left[\frac{1}{2} \log(\cosh^2 2b \operatorname{sech}^2 h + \tanh^2 h) \right] \\ &\times \{ \pi(1 + \cosh 4b + 2 \cosh 2h)^2 \operatorname{sech}^2 h - \operatorname{sech}^2 h - 16 \bar{k} \\ &\times \{ 4 \operatorname{sech}^2 \left[\frac{1}{2} \log(\cosh^2 2b \operatorname{sech}^2 h + \tanh^2 h) \right] \times \tanh^2 \left[\frac{1}{2} \log(\cosh^2 2b \operatorname{sech}^2 h + \tanh^2 h) \right] \} \\ &\times (\cosh 4b + \cosh 2h - 8 \cosh^4 b \operatorname{sech}^2 h \sinh 4b) \} \sinh 4b, \end{aligned} \quad (\text{A.2})$$

$$\begin{aligned} \frac{\partial f_2}{\partial h} &= \frac{1}{16\pi(\cosh 4b + \cosh 2h)^2} \operatorname{csch} \left[\frac{1}{2} \log(\cosh^2 2b \operatorname{sech}^2 h + \tanh^2 h) \right] \\ &\times \operatorname{sech} \left[\frac{1}{2} \log(\cosh^2 2b \operatorname{sech}^2 h + \tanh^2 h) \right] \\ &\times \{ \pi(1 + \cosh 4b + 2 \cosh 2h)^2 \operatorname{sech}^2 h - 16 \bar{k} \{ 4 \operatorname{sech}^2 \left[\frac{1}{2} \log(\cosh^2 2b \operatorname{sech}^2 h + \tanh^2 h) \right] \\ &\times \tanh^2 \left[\frac{1}{2} \log(\cosh^2 2b \operatorname{sech}^2 h + \tanh^2 h) \right] \} (\cosh 4b + \cosh 2h - 8 \cosh^4 b \operatorname{sech}^2 h \sinh 4b) \} \\ &\times \sinh^2 2b \tanh h. \end{aligned} \quad (\text{A.3})$$

where the parameter \bar{k} defines the first type of the elliptic integral.

References

- [1] F. Weinhold, Metric geometry of equilibrium thermodynamics, J. Chem. Phys. **63**, 2479-2483 (1975). doi:10.1063/1.431689
- [2] G. Ruppeiner, Thermodynamics: A Riemannian geometric model, Phys. Rev. A **20**, 1608-1613 (1979). doi:10.1103/PhysRevA.20.1608
- [3] G. Ruppeiner, Riemannian geometry in thermodynamic fluctuation theory, Rev. Mod. Phys. **67**, 605 (1995). doi:10.1103/RevModPhys.67.605

24 REFERENCES

- [4] S. A. H. Mansoori and B. Mirza, Correspondence of phase transition points and singularities of thermodynamic geometry of black holes, *Eur. Phys. J. C* **74**, 2681 (2014). doi:[10.1140/epjc/s10052-013-2681-6](https://doi.org/10.1140/epjc/s10052-013-2681-6)
- [5] S. A. H. Mansoori, B. Mirza, and M. Fazel, Hessian matrix, specific heats, Nambu brackets, and thermodynamic geometry, *JHEP* **2015**, 115 (2015). doi:[10.1007/JHEP04](https://doi.org/10.1007/JHEP04)
- [6] G. Ruppeiner, Thermodynamic curvature measures interactions, *Am. J. Phys.* **78**, 1170 (2010). doi:[10.1119/1.3459936](https://doi.org/10.1119/1.3459936)
- [7] H. Janyszek and R. Mrugaa, Riemannian geometry and stability of ideal quantum gases, *J. Phys. A: Math. Gen.* **23**, 467 (1990). doi:[10.1088/0305-4470/23/4/016](https://doi.org/10.1088/0305-4470/23/4/016)
- [8] B. Mirza and H. Mohammadzadeh, Ruppeiner geometry of Anyon gas, *Phys. Rev. E* **78**, 021127 (2008). doi:[10.1103/PhysRevE.78.021127](https://doi.org/10.1103/PhysRevE.78.021127)
- [9] B. Mirza and H. Mohammadzadeh, Nonperturbative thermodynamic geometry of anyon gas, *Phys. Rev. E* **80**, 011132 (2009). doi:[10.1103/PhysRevE.80.011132](https://doi.org/10.1103/PhysRevE.80.011132)
- [10] G. Ruppeiner, Application of Riemannian geometry to the thermodynamics of a simple fluctuating magnetic system, *Phys. Rev. A* **24**, 488-492 (1981). doi:[10.1103/PhysRevA.24.488](https://doi.org/10.1103/PhysRevA.24.488)
- [11] B. Mirza and Z. Talaei, Thermodynamic geometry of a Kagome Ising model in a magnetic field, *Phys. Lett. A* **377**, 513 (2013). doi:[10.1016/j.physleta.2012.12.030](https://doi.org/10.1016/j.physleta.2012.12.030)
- [12] D. Brody and N. Rivier, Geometrical aspects of statistical mechanics, *Phys. Rev. E* **51**, 1006-1011 (1995). doi:[10.1103/PhysRevE.51.1006](https://doi.org/10.1103/PhysRevE.51.1006)
- [13] D. C. Brody and A. Ritz, Information geometry of finite Ising models, *J. Geom. Phys.* **47**, 207-220 (2003). doi:[10.1016/S0393-0440\(02\)00190-0](https://doi.org/10.1016/S0393-0440(02)00190-0)
- [14] T. Nakamura, Scalar Curvature of the Quantum Exponential Family for the Transverse-Field Ising Model and the Quantum Phase Transition, (2022). doi:[10.48550/arXiv.2212.12919](https://doi.org/10.48550/arXiv.2212.12919)
- [15] D. A. Johnston, W. Janke, and R. Kenna, Information geometry, one, two, three (and four), *Acta Phys. Pol. B* **34**, 4923-4937 (2003). doi:[10.48550/arXiv.cond-mat/0308316](https://doi.org/10.48550/arXiv.cond-mat/0308316)
- [16] S. A. H. Mansoori and B. Mirza, Geometrothermodynamics as a singular conformal thermodynamic geometry, *Phys. Lett. B* **799**, 135040 (2019). doi:[10.1016/j.physletb.2019.135040](https://doi.org/10.1016/j.physletb.2019.135040)
- [17] B. Mirza, M. Zamaninasab, Ruppeiner geometry of RN black holes flat or curved? *JHEP* **1006**, 059 (2007). doi:[10.1088/1126-6708/2007/06/059](https://doi.org/10.1088/1126-6708/2007/06/059)
- [18] G. Ruppeiner, Thermodynamic curvature and phase transitions in Kerr-Newman black holes, *Phys. Rev. D* **78**, 024016-1-13 (2008). doi:[10.1103/PhysRevD.78.024016](https://doi.org/10.1103/PhysRevD.78.024016)
- [19] D. Kubiznak and R. B. Mann, P-V criticality of charged AdS black holes, *J. High Energy Phys.* **1207**, 033 (2012). doi:[10.1007/JHEP07\(2012\)033](https://doi.org/10.1007/JHEP07(2012)033)

- [20] B. Mirza and Z. Sherkatghanad, Phase transitions of hairy black holes in massive gravity and thermodynamic behavior of charged AdS black holes in an extended phase space, *Phys. Rev. D* **90**, 084006 (2014). [doi:10.1103/PhysRevD.90.084006](https://doi.org/10.1103/PhysRevD.90.084006)
- [21] S. A. H. Mansoori, M. Rafiee, and S.-W. Wei, Universal criticality of thermodynamic curvatures for charged AdS black holes, *Phys. Rev. D* **102**, 124066 (2020). [doi:10.1103/PhysRevD.102.124066](https://doi.org/10.1103/PhysRevD.102.124066)
- [22] S. A. H. Mansoori, B. Mirza, and E. Sharifian, Extrinsic and intrinsic curvatures in thermodynamic geometry, *Phys. Lett. B* **759**, 298-305 (2016). [doi:10.1016/j.physletb.2016.05.096](https://doi.org/10.1016/j.physletb.2016.05.096)
- [23] P. Salamon, et al. On the relation between entropy and energy versions of thermodynamic length, *J. Chem. Phys.* **80**, 436-437 (1984). [doi:10.1063/1.446467](https://doi.org/10.1063/1.446467)
- [24] F. Wilczek, Quantum mechanics of fractional-spin particles, *Phys. Rev. Lett.* **49**, 957 (1982). [doi:10.1103/PhysRevLett.49.957](https://doi.org/10.1103/PhysRevLett.49.957)
- [25] F. D. M. Haldane, Fractional statistics in arbitrary dimensions: a generalization of the Pauli principle, *Phys. Rev. Lett.* **67**, 937 (1991). [doi:10.1103/PhysRevLett.67.937](https://doi.org/10.1103/PhysRevLett.67.937)
- [26] J. M. Leinaas and J. Myrheim, On the theory of identical particles, *Nuovo Cimento Soc. Ital. Fis.*, **37B**, 1 (1977).
- [27] Y.-S. Wu, Statistical Distribution of Particles obeying Fractional Statistics, *Phys. Rev. Lett.* **73**, 922 (1994). [doi:10.48550/arXiv.cond-mat/9402008](https://doi.org/10.48550/arXiv.cond-mat/9402008)
- [28] C. N. Yang and C.P. Yang, Thermodynamics of a one-dimensional system of bosons with repulsive delta-function interaction, *J. Math. Phys.* **10**, 1115 (1969). [doi:10.1063/1.1664947](https://doi.org/10.1063/1.1664947)
- [29] G. S. Canright and S. M. Girvin, Fractional Statistics: Quantum Possibilities in Two Dimensions, *Science* **247**, 1197 (1990). [doi:10.1126/science.247.4947.1197](https://doi.org/10.1126/science.247.4947.1197)
- [30] M. Chaichian, R. Gozales Felipe, and C. Montonen, Statistics of q-oscillators, quons and relations to fractional statistics, *J. Phys. A* **26**, 4017 (1993). [doi:10.1088/0305-4470/26/16/018](https://doi.org/10.1088/0305-4470/26/16/018)
- [31] M. V. N. Murthy and R. Shankar, Thermodynamics of a one-dimensional ideal gas with fractional exclusion statistics, *Phys Rev. Lett.* **73**, 3331 (1994). [doi:10.1103/PhysRevLett.73.3331](https://doi.org/10.1103/PhysRevLett.73.3331)
- [32] C. Nayak and F. Wilczek, Exclusion statistics: Low-temperature properties, fluctuations, duality, and applications, *Phys. Rev. Lett.* **73**, 2740 (1994). [doi:10.1103/PhysRevLett.73.2740](https://doi.org/10.1103/PhysRevLett.73.2740)
- [33] F. M. D. Pellegrino, G. G. N. Angilella, N. H. March and R. Pucci, Statistical correlations in an ideal gas of particles obeying fractional exclusion statistics, *Phys. Rev. E* **76**, 061123 (2007). [doi:10.1103/PhysRevE.76.061123](https://doi.org/10.1103/PhysRevE.76.061123)
- [34] S. Vishveshwara, M. Stone and D. Sen, Correlators and fractional statistics in the quantum hall bulk, *Phys. Rev. Lett.* **99**, 190401 (2007). [doi:10.1103/PhysRevLett.99.190401](https://doi.org/10.1103/PhysRevLett.99.190401)
- [35] W.-H. Huang, Boson-fermion transmutation and the statistics of anyons, *Phys.*

- Rev. E **51**, 3729 (1995). doi:10.1103/PhysRevE.51.3729
- [36] W.-H. Huang, Statistics of anyon gas and the factorizable property of thermodynamic quantities, *Phys. Rev. B* **53**, 15842 (1996). doi:10.1103/PhysRevB.53.15842
- [37] W.-H. Huang, Comment on Quantum Statistical Mechanics of an Ideal Gas with Fractional Exclusion Statistics in Arbitrary Dimension, *Phys. Rev. Lett.* **81**, 2392 (1998). doi:10.1103/PhysRevLett.81.2392.
- [38] G. Baxter, Weight Factors for the Two-Dimensional Ising Model, *J. Math. Phys.* **6**:1015 (1965). doi:10.1063/1.1704362
- [39] B. M. McCoy and T. T. Wu, Theory of Toeplitz determinants and the spin correlations of the two-dimensional Ising model. II, *Phys. Rev.* **155** (2): 438 (1967). doi:10.1103/PhysRev.155.438
- [40] M. E. Fisher, Lattice statistics in a magnetic field, I. A two-dimensional superexchange antiferromagnet, *Proc. of the Royal Society, A*, **254**, 66 (1960). doi:10.1098/rspa.1960.0005
- [41] R. J. Baxter, *Exactly Solved Models in Statistical Mechanics* (Academic: New York 1982).
- [42] P. Azaria and H. Giacomini, An exactly solvable two-dimensional Ising model with magnetic field, *J. Phys. A* **21**, L935 (1988). doi:10.1088/0305-4470/21/19/003
- [43] K. Y. Lin, An exact result for the magnetisation of the Kagome lattice Ising model with magnetic field, *J. Phys. A* **22**, 3435 (1989). doi:10.1088/0305-4470/22/16/033
- [44] W. T. Lu, F. Y. Wu, Soluble kagome Ising model in a magnetic field, *Phys. Rev. E* **71**, 046120 (2005). doi:10.1103/PhysRevE.71.046120
- [45] R. M. F. Houtappel, Order-disorder in hexagonal lattices, *Physica* **16**, 425-455 (1950). doi:10.1016/0031-8914(50)90130-3
- [46] I. Syozi, C. Domb and M. S. Green, *Phase Transitions and Critical Phenomena* ((Academic Press, New York 1972).
- [47] M. E. Khuzani, B. Mirza, and M. T. Kachi, Thermodynamic geometry of pure Lovelock black holes, *Int. J. Mod. Phys. D.* **31**, 2250097 (2022). doi:10.1142/S0218271822500973
- [48] T. Berlin and M. Kac, The Spherical Model of a Ferromagnet, *Phys. Rev.* **86** 821 (1952). doi:10.1103/PhysRev.86.821
- [49] D. V. Boulatov and V.A. Kazakov, The ising model on a random planar lattice: The structure of the phase transition and the exact critical exponents , *Phys. Lett. B* **186** (1987). doi:10.1016/0370-2693(87)90312-1
- [50] W. Janke, D. A. Johnston, and Ranasinghe P.K.C. Malmimi, The Information Geometry of the Ising Model on Planar Random Graphs, *Phys. Rev. E.* **186** (2002). doi:10.1103/PhysRevE.66.056119
- [51] W. Janke, D. A. Johnston, and R. Kenna, Information geometry of the spherical model, *Phys. Rev. E* **67**, 046106, (2003). doi:10.1103/PhysRevE.67.046106

- [52] H. Janyszek, Riemannian geometry and stability of thermodynamical equilibrium systems, *J. Phys. A* **23**, 477 (1990). [doi:10.1088/0305-4470/23/4/017](https://doi.org/10.1088/0305-4470/23/4/017)